

## The IMF dependence of the local time of transpolar arcs: Implications for formation mechanism

R. C. Fear<sup>1</sup> and S. E. Milan<sup>1</sup>

Received 29 September 2011; revised 21 December 2011; accepted 22 January 2012; published 13 March 2012.

[1] Transpolar arcs are auroral features that extend from the nightside auroral oval into the polar cap. It is well established that they occur predominantly when the interplanetary magnetic field (IMF) has a northward component ( $B_z > 0$ ). Results concerning how the magnetic local time at which transpolar arcs form might depend upon the IMF dawn-dusk component ( $B_Y$ ) are more mixed. Some studies have found a correlation between these two variables, with Northern Hemisphere arcs forming predominantly premidnight when  $B_Y > 0$  and postmidnight when  $B_Y < 0$  and vice versa in the Southern Hemisphere. However, a more recent statistical study found that there was no significant correlation, and other studies find that the formation of moving arcs is triggered by a change in the sign of the IMF  $B_Y$  component. In this paper, we investigate the relationship between the magnetic local time at which transpolar arcs form and the IMF  $B_Y$  component. It is found that there is indeed a correlation between the magnetic local time at which transpolar arcs form and the IMF  $B_Y$  component, which acts in opposite senses in the Northern and Southern hemispheres. However, this correlation is weak if the IMF is only averaged over the hour before the first emergence of the arc and becomes stronger if the IMF is averaged 3–4 h beforehand. This is consistent with a mechanism where the magnetic local time at which the arc first forms depends on the  $B_Y$  component in the magnetotail adjacent to the plasma sheet, which is determined by the IMF  $B_Y$  component during intervals of dayside reconnection in the hours preceding the first emergence of the arc. We do not find evidence for the triggering of arcs by an IMF  $B_Y$  sign change.

**Citation:** Fear, R. C., and S. E. Milan (2012), The IMF dependence of the local time of transpolar arcs: Implications for formation mechanism, *J. Geophys. Res.*, 117, A03213, doi:10.1029/2011JA017209.

### 1. Introduction

[2] This paper studies the formation of transpolar arcs (TPA), which can potentially shed light on the complex magnetic topology that the magnetosphere can attain during prolonged periods of northward IMF. The main region of auroral emission in each hemisphere is the main auroral oval, which encircles the magnetic pole, and is situated on closed magnetic field lines. The auroral ovals encircle the polar caps, which are the regions of open magnetic flux which map out to the lobes. Auroral arcs can occasionally be observed poleward of the main auroral oval; ground-based observations provide information about the small-scale structure of these auroral structures, and it has been observed that they are often aligned in the direction of the Sun [Mawson, 1925, pp. 178–182; Weill, 1958]. Consequently, they are variously referred to as polar cap arcs, Sun-aligned arcs or high-latitude auroras. Statistical studies have shown

that occurrence of high-latitude auroras is anticorrelated with magnetic activity [Davis, 1963], and that they occur predominantly during intervals when the interplanetary magnetic field (IMF) has a northward component [Berkey *et al.*, 1976; Gussenhoven, 1982]. The first global-scale satellite observations of the polar region revealed that similar arcs occur on a large scale, forming such that they sometimes connect the dayside and nightside of the auroral oval [Frank *et al.*, 1982], which are termed transpolar arcs or theta aurora. Observations from low-altitude spacecraft above transpolar arcs have shown that the plasma above transpolar arcs is similar in composition and density to plasma above the poleward edge of the main auroral oval, and consistent with a plasma sheet origin, strongly suggesting that transpolar arcs are on closed magnetic field lines embedded within the open field lines of the polar cap [Peterson and Shelley, 1984; Frank *et al.*, 1986]. In this paper we shall use the general term “polar cap arc” when referring to models of generic auroral features observed within the polar cap, and “transpolar arc” to refer specifically to a large-scale arc within the polar cap (which may or may not form a complete “theta”). Ground-based observations and some of the early satellite-based observations are limited in their field of view; it is not entirely clear whether all ground-based

<sup>1</sup>Department of Physics and Astronomy, University of Leicester, Leicester, UK.

observations of polar cap arcs are in fact observations of part of a transpolar arc or whether they are driven by different processes. Therefore, in the remainder of this introduction we draw attention to the type of observation used in each study.

[3] It seems reasonably clear that the IMF  $B_Y$  component influences the direction of motion of polar cap arcs. *Craven and Frank* [1991] observed that in the small number of previously published studies of globally imaged transpolar arcs, those which occurred in the Northern Hemisphere had a dawnward motion when  $B_Y$  was negative, and duskward motion when  $B_Y$  was positive. *Craven et al.* [1991] reported the first simultaneous observations of a transpolar arc in both the northern and Southern Hemisphere, and reported opposite directions of motion in the two hemispheres. However, *Valladares et al.* [1994] (studying 150 polar cap arcs observed in all-sky camera images) found this simple picture was complicated by a further dependence upon the location of the arc within the polar cap, at least for the smaller-scale arcs imaged from the ground. They concluded there were two effects: (1) a motion dictated by  $B_Y$  as a result of the expansion of the dusk or dawn convection cell (depending upon the sign of  $B_Y$ ) relative to the polar cap and (2) a motion toward the noon/midnight meridian for some events as a result of the overall contraction of the polar cap when reconnection occurs in the magnetotail. Recently *Hosokawa et al.* [2011] examined 743 polar cap arcs observed by an all-sky imager, and found that arcs with motion which followed the trend observed by *Craven and Frank* [1991] also moved faster if the magnitude of  $B_Y$  was larger. *Hosokawa et al.* [2011] concluded that these arcs were in a region where the polar cap convection was affected by  $B_Y$  (either on open magnetic field lines, or in the closed magnetosphere adjacent to the open-closed boundary). However, the arcs whose motion was uncorrelated with  $B_Y$  always moved toward the noon/midnight meridian. *Hosokawa et al.* [2011] concluded that these arcs were situated on closed magnetic field lines on the flank, and were not connected to the magnetotail plasma sheet.

[4] Observations of a correlation between the IMF  $B_Y$  component and the local time dependence at which polar cap arcs form have provided mixed results. Some statistical studies [e.g., *Gussenhoven*, 1982; *Gusev and Troshichev*, 1986] have found a dependence. *Gussenhoven* [1982] examined satellite images of Northern Hemisphere aurora at very high magnetic latitudes (above  $80^\circ$ ) and found that postmidnight arcs tended to occur more often when  $B_Y$  was negative in the hour before the arc was observed, and pre-midnight arcs preferentially occurred when  $B_Y$  was positive. Since the IMF frequently changes orientation, *Gussenhoven* [1982] repeated their analysis with the subset of events where the IMF clock angle remained in the same quadrant for 2 h before the time of the image, and found the same  $B_Y$ /local time dependence. *Gusev and Troshichev* [1986] reported the opposite trend in the Southern Hemisphere based on all-sky camera images of hook-shaped polar cap arcs observed in the dayside sector during the austral winter. Conversely, *Valladares et al.* [1994] did not find a clear  $B_Y$  dependency on the side of the polar cap at which the arcs were located. (They attributed this in part to selection criteria; their observations were mainly of weak polar cap arcs,

which may not make up a significant proportion of events in satellite-based studies.) *Kullen et al.* [2002] presented the first, and so far only statistical study of globally imaged transpolar arcs. They identified 74 clear polar cap arcs which lasted for longer than 10 min, were clearly separated from the auroral oval and where the observational field of view and strength of emissions were sufficient to establish its evolution. (They also identified a further 146 “small split” events which were either short-lived, or were not distinct enough from the auroral oval to exclude the possibility that the arc was an oval-related arc.) *Kullen et al.* [2002] did not explicitly report the dependence of the arc location on the IMF evaluated before the start of each arc, but they compared the locations of the arcs with the mean IMF  $B_Y$  component observed during the lifetime of the arc and with the  $B_Y$  component at the event start time, and investigated whether any of the IMF components changed sign in the hour preceding the first observation of the arc. (Some previous case studies had associated the side of the polar cap in which arcs form with changes in the IMF  $B_Y$  component [*Cumnock et al.*, 1997; *Cumnock and Blomberg*, 2004].) They found that the clear arcs which formed in the Northern Hemisphere near the dawnside or duskside oval and did not have any significant subsequent motion generally did not coincide with a  $B_Y$  sign change, and occurred mainly pre-midnight when  $B_Y > 0$  and postmidnight for  $B_Y < 0$  (consistent with *Gussenhoven* [1982]). However, arcs which moved across the polar cap were mostly associated with a  $B_Y$  sign change in the hour beforehand; the six arcs that were first observed postmidnight had an average positive  $B_Y$  component during the lifetime of the arc, and the four pre-midnight arcs were evenly split between positive and negative  $B_Y$ . By implication, the dependence would be similar to that observed by *Gussenhoven* [1982] if the IMF was averaged before the arc was observed. Therefore, *Kullen et al.* [2002] concluded that moving arcs were triggered by a change in the  $B_Y$  component. Their findings will be discussed in further detail in section 2. At this point, we note that with the exception of the steady IMF cases examined by *Gussenhoven* [1982], no previous studies of the local time of polar cap arc formation have examined the IMF more than 1 h before the first observation of the arc. (*Kullen et al.* [2002] did examine the mean IMF components for several hours beforehand to determine what IMF orientations were associated with different classifications of arc, but did not compare location at which arcs formed with the IMF prior to the arc beyond the analysis described above.)

[5] In this paper, we present evidence for a dependence of the magnetic local time at which transpolar arcs first emerge on the IMF  $B_Y$  component, consistent with the observations of *Gussenhoven* [1982], based on a new survey of transpolar arcs observed by the IMAGE satellite FUV cameras. However, we find that the correlation is strongest if the IMF is averaged not over the preceding hour or two (as per *Gussenhoven* [1982]) or during the lifetime of the arc [*Kullen et al.*, 2002], but if the IMF is considered 3–4 h before the first emergence of the arc. This time scale is consistent with the time expected for newly opened magnetospheric flux at the dayside to reach the inside edge of the lobe, adjacent to the magnetotail plasma sheet, as described by the Dungey cycle of magnetospheric convection [*Dungey*,

1961]. Therefore, it is indicative of the driver of transpolar arc formation being based in the plasma sheet, consistent with the plasma observations discussed above [Peterson and Shelley, 1984; Frank et al., 1986]. We only discuss the effects of the IMF, as this is the only parameter for which there is a theoretical basis to explain variation in the location at which arcs form. We emphasize at the outset that we are concerned here with the  $B_Y$  control of the location within the polar cap at which transpolar arcs first form, and not with any  $B_Y$  control of the subsequent motion of the arcs. These two effects may well be driven by different processes [e.g., Milan et al., 2005].

[6] In section 2, we will provide an overview of various models which have been proposed for the formation of polar cap arcs (including transpolar arcs), and summarize the predictions they make for a  $B_Y$  dependence upon the local time at which the arcs form. This will be followed by a description of the instrumentation used in this study and the compilation of our own list of transpolar arcs (section 3). In section 4, we present the IMF dependence of the location at which those arcs first emerge, followed by a discussion of our results and conclusions.

## 2. Previously Proposed Models

[7] Several models have been proposed to explain the formation of polar cap arcs, which are discussed in a review paper by Zhu et al. [1997]. The earliest models did not consider the effects of an IMF  $B_Y$  component. Burke et al. [1982] proposed that the arcs could be formed by electron precipitation on open magnetic field lines, caused by a diversion of a small proportion of the magnetopause current along field-aligned currents into the ionosphere. Frank et al. [1982] suggested that transpolar arcs could be formed as a consequence of a bifurcation of the lobe, and others have proposed models based on magnetopause reconnection tailward [Kan and Burke, 1985] or sunward [Toffoletto and Hill, 1989] of the cusps, providing a channel of closed flux within the polar cap. (However, since the Kan and Burke [1985] model invokes reconnection between the magnetosheath magnetic field and closed magnetotail flux, then this would require the lobes to be entirely eroded by dual lobe reconnection first: a situation which only occurs when the IMF is strongly northward for several hours [Fairfield et al., 1996; Newell et al., 1997].)

[8] The models which take account of the IMF  $B_Y$  component are summarized in Table 1, which indicates the predictions made for the location of polar cap arcs for positive and negative IMF  $B_Y$  components. They invoke a variety of mechanisms. Some relate the arcs to the three- or four-cell convection pattern that arises when reconnection occurs between the magnetosheath and magnetospheric magnetic fields when the IMF is northward [Chiu et al., 1985; Lyons, 1985; Sojka et al., 1994]. Lyons [1985] and Sojka et al. [1994] predicted that the sign of  $B_Y$  should control whether arcs were formed in the Northern or Southern Hemisphere. Chiu et al. [1985] predicted arcs in both hemispheres, but that the arc in one hemisphere should be on open field lines with plasma originating in the magnetosheath, while the arc in the other hemisphere should be on closed field lines with plasma originating in the plasma sheet. Since the driver for the required flows is reconnection poleward of the cusp, one

would expect the IMF  $B_Y$  component to have a reasonably prompt influence on the local time at which an arc subsequently forms.

[9] Three models [Newell and Meng, 1995; Chang et al., 1998; Kullen, 2000] attribute polar cap arcs to a sudden change in the IMF. Newell and Meng's [1995] model places arcs initially at the poleward edge of the dawn or dusk side of the auroral oval (when the IMF is northward), and the arc then detaches and moves into the polar cap when the IMF turns southward. Chang et al. [1998] extended the Newell and Meng [1995] model and predicted that arcs could also form if the IMF remained northward but the sign of the  $B_Y$  component changed. While we do not aim to provide a detailed critique of each model in this section, we do note that the Chang et al. [1998] model is unrealistic as it requires the new magnetopause reconnection site to map to a point in the ionosphere that is equatorward of the open-closed boundary, trapping some closed flux between the newly opened flux and polar cap. (By definition, the outermost closed magnetospheric field line and the most recently opened magnetic field line map to points immediately either side of the open-closed boundary.) Both of these models are driven by reconnection at the magnetopause, and the change in the IMF orientation is an explicit requirement, so both models would produce arcs promptly after a rotation in the IMF. The Kullen [2000] model differed slightly in that the IMF rotation introduced a twist into the magnetotail. (Fairfield [1979] observed that the cross-tail [ $B_Y$ ] component of the magnetotail magnetic field was correlated with the IMF  $B_Y$  component. This was explained by Cowley [1981] as due to the tension exerted by the IMF on newly opened dayside magnetic field lines which are added to the lobe.) Kullen [2000] modeled this twist by adding a  $B_Y$  component to the Tsyganenko [1989] model magnetotail magnetic field. The added  $B_Y$  component was positive at the Earthward end of the magnetotail, to represent a currently positive IMF  $B_Y$  orientation, and negative further downtail, to represent an earlier negative  $B_Y$  orientation. The interface in the magnetotail between the two twist regions was propagated antisunward as the interface in the solar wind between the two different regions also moved tailward. Kullen [2000] then mapped the magnetotail plasma sheet through the twist interface to the ionosphere. This process gave rise to a patch of closed flux in the polar cap which formed on the morning side of the auroral oval and then moved across the polar cap. It was argued that the response to an IMF rotation should be prompt, as the modeled arc was noticeably detached by the time the interface (both in the magnetotail and in the solar wind) was  $25 R_E$  downtail of the terminator. The motion of the arc was a direct consequence of the tailward propagation of the rotation front; therefore this model can only explain moving arcs. In this model, the response time is determined by the speed at which the rotation front travels down the magnetotail, and the presence of the arc in the model is a consequence of the manner in which the IMF rotation is applied to the magnetotail (initially applied uniformly though a cross section of the tail at the Earthward end, and then propagated antisunward). Such an application does differ from the theoretical picture proposed by Cowley [1981]. The cross-tail component described by Cowley [1981] is initially added to the outside edge of the lobe, but as dayside and nightside reconnection continue,

**Table 1.** A Summary of the Models That Have Been Proposed for Transpolar Arc Formation and That Make a Prediction for an IMF  $B_Y$  Control of the Location at Which the Arcs Form<sup>a</sup>

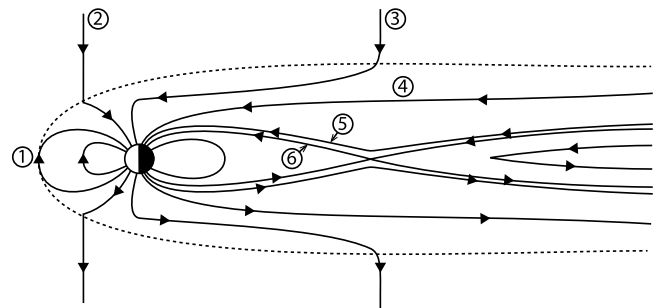
Model	Mechanism	Location of Arcs if		Interaction Region	Response to IMF	Notes
		$B_Y < 0$	$B_Y > 0$			
		Prior to First Emergence				
<i>Chiu et al.</i> [1985]	Field-aligned current structure related to reverse convection and three/four-cell convection pattern	NH: Postmidnight at or near OCB SH: Center of polar cap or postmidnight	NH: Postmidnight or near center of polar cap SH: Postmidnight, at or near OCB	Magnetopause, tailward of cusp	Reasonably prompt (magnetopause driver)	Source of plasma (magnetosheath or plasma sheet) differs depending upon sign of $B_Y$ and hemisphere
<i>Lyons</i> [1985]	Field-aligned current structure related to reverse convection and three/four-cell convection pattern	Mostly in SH	Mostly in NH	Magnetopause, tailward of cusp	Reasonably prompt (magnetopause driver)	Polar cap aurora should not generally be observed simultaneously in both hemispheres
<i>Reiff and Burch</i> [1985]	Closure of magnetotail flux	$B_X < 0$ : Postmidnight in NH and SH; moving toward center in SH $B_X > 0$ : Premidnight in NH and SH; moving toward center in NH	$B_X < 0$ : Premidnight in NH and SH; moving toward center in SH $B_X > 0$ : Postmidnight in NH and SH; moving toward center in NH	Magnetotail	Delayed by time for opened lobe flux to convect to position where it can reclose	
<i>Makita et al.</i> [1991]	Asymmetric main auroral oval caused by tilt or dawn/dusk asymmetry in plasma sheet	NH: Postmidnight, at poleward edge of morning side of oval SH: Depends on whether plasma sheet is tilted or asymmetric	NH: Premidnight, at poleward edge of evening side of oval SH: Depends on whether plasma sheet is tilted or asymmetric	Magnetotail	Delayed by time taken for flux to transport to layer adjacent to magnetotail current sheet	Cannot explain arcs away from dawn or dusk side of main oval, or motion across polar cap
<i>Sofka et al.</i> [1994]	Field-aligned currents caused by shear flow in three-cell convection pattern imposed on ionosphere	Mainly in SH, in center of polar cap	Mainly in NH, in center of polar cap	Magnetopause, tailward of cusp	Reasonably prompt (magnetopause driver)	
<i>Newell and Meng</i> [1995]	Arcs form at flow shears near OCB when $B_Z > 0$ ; arc detaches from main oval after IMF turns southward		NH: Form postmidnight and move duskward SH: Form premidnight and move dawnward	Magnetopause	Promptly follows IMF southward turn	If IMF turns northward again, motion of arc ceases
<i>Rezhenov</i> [1995]	Plasma sheet instability causing tailward motion of a "tongue" of plasma sheet plasma	Emerges near midnight, but develops toward postmidnight side (NH) or premidnight side (SH)	Emerges near midnight, but develops toward premidnight side (NH) or postmidnight side (SH)	Magnetotail	Follows substorm recovery or soon after northward turning of IMF	

Table 1. (continued)

Model	Mechanism	Location of Arcs if		Interaction Region	Response to IMF	Notes
		$B_y < 0$	$B_y > 0$			
<i>Chang et al.</i> [1998]	Change in reconnection site after change in sign of $B_z$ or $B_y$	NH: Premidnight <sup>b</sup> SH: Postmidnight <sup>b</sup>	NH: Postmidnight <sup>b</sup> SH: Premidnight <sup>b</sup>	Magnetopause	Prompt response to change in $B_z$ and/or $B_y$	See explanatory note below <sup>b</sup>
<i>Kuiten</i> [2000]	Introduction of a twist into the magnetotail	NH: Premidnight <sup>b</sup> SH: Postmidnight <sup>b</sup>	NH: Postmidnight <sup>b</sup> SH: Premidnight <sup>b</sup>	Magnetotail	Reasonably prompt; arc appears when IMF rotation front is $1.5 R_E$ downtail in solar wind	Explains only moving arcs; see explanatory note below <sup>b</sup>
<i>Milan et al.</i> [2005]	Magnetotail reconnection in twisted magnetotail	NH: Postmidnight SH: Premidnight	NH: Premidnight SH: Postmidnight	Magnetotail	Delayed by time taken for flux to transport to layer adjacent to magnetotail current sheet	

<sup>a</sup>NH, Northern Hemisphere; SH, Southern Hemisphere.

<sup>b</sup>The predicted locations noted for the *Chang et al.* [1998] and *Kuiten* [2000] models are based on the sign of  $B_y$  immediately before the arc becomes distinctly observable, and therefore just after the change of sign in  $B_y$ . Consequently, if the location is compared with the IMF an hour or two before the start of the arc, then the opposite relationship should be observed (i.e., the same dependence as predicted by the *Milan et al.* [2005] model).



**Figure 1.** A cross-sectional view of the magnetosphere, indicating the necessity of a long time delay when trying to correlate the IMF  $B_y$  component with plasma sheet processes. The dotted line indicates the magnetopause. Magnetic field line 1 is the outermost closed field line on the dayside magnetosphere. Field lines 2–5 are open lobe field lines that map into the polar cap. Field line 2 is the most recently opened field line. Field line 3 has been drawn such that it maps to the IMF part of the field line at about the same distance downtail as the magnetotail reconnection line. If the solar wind transit time had been used to propagate an IMF rotation downtail, then 3, which only maps through the outer part of the lobe, is the most tailward field line that adopts the new  $B_y$  orientation. Field line 4 is currently undergoing reconnection in the tail; therefore 5 will be the next field line to undergo reconnection. Note that 5 crosses the magnetopause and maps into the solar wind a long way farther downtail than 3.

the field line that has been added to the edge of the lobe moves closer toward the plasma sheet, until it is adjacent to the plasma sheet and becomes the next field line to be closed by reconnection, as sketched in Figure 1 based on the open magnetosphere model proposed by *Dungey* [1961]. A similar process has been observed in MHD simulations: *Walker et al.* [1999] reported that the twist is added at a given location just inside the tail magnetopause shortly after the IMF rotation arrives at that location, but the response time is much longer closer to the plasma sheet.

[10] Several proposed mechanisms link polar cap arcs to the plasma sheet or to magnetotail processes. As in some of the mechanisms discussed above, *Reiff and Burch* [1985] also linked the formation of transpolar arcs to flow patterns in the ionosphere, but their mechanism invoked single-lobe reconnection between the IMF and open flux on the outward edge of the lobe occurring simultaneously in both hemispheres, the subsequent tailward motion of the field lines in both hemispheres (corresponding to an antisunward motion of its footprint in the polar cap) and the closure of the open field lines downtail. *Makita et al.*'s [1991] mechanism attributed polar cap arcs on the morning/evening side of the polar cap to an asymmetric main auroral oval, which was thickened on one side by either a tilted magnetotail plasma sheet, or a plasma sheet which was thicker on one side of the magnetotail than the other. However, the *Makita et al.* [1991] mechanism can only explain arcs which form at the poleward edge of the dawn or dusk side of the main oval and remain there, not arcs which form near midnight or which move across the polar cap. *Rezhnev* [1995] proposed a mechanism whereby plasma from the plasma sheet

boundary layer is displaced tailward onto other magnetic field lines which map further poleward in the ionosphere. The magnetotail configuration envisaged by *Rezhnev* [1995] is somewhat unlikely, since the plasma sheet is required to lie “deep inside” the region of closed magnetic field lines and the open-closed field line boundary lies significantly poleward of the poleward edge of the main auroral oval. However, in this mechanism, the arcs formed near midnight but extended toward the premidnight or postmidnight side of the polar cap, depending on the IMF  $B_Y$  component. *Milan et al.* [2005] proposed that transpolar arcs were formed by reconnection in the magnetotail following a period of magnetopause reconnection during which the IMF has a  $B_Y$  component, introducing a  $B_Y$  component into the magnetotail as described above [*Fairfield*, 1979; *Cowley*, 1981]. In the *Milan et al.* [2005] mechanism, the transpolar arc is formed because newly closed flux in the magnetotail which crosses the magnetic equator near midnight magnetic local time (MLT) has a premidnight footprint in one hemisphere and a postmidnight footprint in the other, due to the magnetotail  $B_Y$  component. The authors proposed that the return flow of these newly closed field lines would be hindered and there would be a buildup of closed flux that protrudes into the polar cap. The arc forms on the night side of the oval, and is then predicted to move in response to the “stirring” of lobe flux by subsequent reconnection between the magnetosheath and lobe magnetic fields.

[11] In the *Makita et al.* [1991] and *Milan et al.* [2005] models, the magnetic field which dictates the location at which arcs form is the lobe magnetic field immediately outside the magnetotail plasma sheet. This is determined by the IMF several hours beforehand, as the time scale for a newly opened field line to reach the plasma sheet is expected to be of the order of hours. The time scale can be determined in two separate ways, which we will discuss with reference to the sketch in Figure 1. Magnetospheric magnetic field lines and connected IMF field lines are numbered 1–6. Field line 1 is the outermost closed field line on the dayside, and field line 6 is newly closed on the night side. Therefore, the poleward edges of the auroral oval on the dayside and nightside are given by the ionospheric footprints of 1 and 6, respectively. The first means to calculate the time scale for a magnetic field line to move from 1 to 6 is to use figures quoted by *Dungey* [1965], who estimated that the distance between the poleward edges of the dayside and nightside oval was approximately  $1 R_E$ , and that the open field line moves at speeds of the order of hundreds of meters per second. Therefore the journey of a field line from 1 to 6 takes of the order of 4 h (whether one considers the ionospheric footprint or any other point on the field line). Second, *Milan et al.* [2007] found that the mean open flux in the lobe or polar cap prior to a substorm was 0.6 GWb, and that each substorm closed on average 0.3 GWb of flux. Therefore, approximately two substorms are needed to refresh the flux in the lobe. Since the typical substorm recurrence time is approximately 2.75 h [*Borovsky et al.*, 1993; *Milan et al.*, 2007], this gives rise to an estimate of 5.5 h. Some studies of substorms and transpolar arcs use much shorter time scales to propagate the IMF  $B_Y$  component to the nightside reconnection line, such as the transit time for an IMF field line from the dayside to the nightside reconnection line. Short time scales are reasonable estimates

when considering the response time to effects such as pressure changes [*Craven et al.*, 1986; *Boudouridis et al.*, 2003; *Milan et al.*, 2004], as the effect of a pressure front can travel transverse to the magnetospheric magnetic field. However, the physical justification for such a short time scale for a  $B_Y$  component to become established in the inner lobe seems unclear in the context of the *Dungey* [1961] picture. If the solar wind propagation time to the tail neutral line was used to estimate the state of the magnetosphere in Figure 1, then field line 3 would be the most tailward field line to adopt the new  $B_Y$  orientation despite the fact that it only maps through the outer lobe. Field line 5, which is the next field line that will undergo reconnection in the magnetotail, is connected to the IMF much further downtail. Indeed, *Milan et al.* [2010] compared the IMF  $B_Y$  component with the local time of substorm onsets, and found that the IMF  $B_Y$  component must be positive or negative for several hours prior to substorm onset to influence the local time of the onset.

[12] In their statistical study of transpolar arcs, *Kullen et al.* [2002] concluded that three different models of transpolar arcs were necessary to explain the local time dependencies upon the IMF  $B_Y$  component that they observed. They classified their clear polar cap arcs into five categories: (1) moving arcs were those which moved across the entire polar cap unless they faded out of view beforehand; both the dayside and nightside oval connection points were required to move (11 arcs); (2) bending arcs were those where the sunward end of the arc separated from the main oval and moved while the antisunward end remained fixed (22 arcs); (3) midnight arcs developed from a large bulge in the nightside auroral oval, and then stretched out into the polar cap, possibly reaching the dayside oval and often then moving toward one side of the oval (6 arcs); (4) oval-aligned arcs appeared near the dawnside or duskside oval, but had no significant motion before they disappeared (28 arcs); and (5) the remaining 7 events were multiple arcs. The oval-aligned arcs occurred mostly on the dusk side when  $B_Y > 0$  and on the dawn side when  $B_Y < 0$ , which was argued to be consistent with the *Makita et al.* [1991] model, and midnight arcs were attributed to the *Rezhnev* [1995] model. Nine out of the eleven moving arcs were associated with a change in sign of the IMF  $B_Y$  component during the period starting 60 min before the arc was first observed and ending 10 min afterward (a much higher proportion than in the other categories of arc). Therefore, *Kullen et al.* [2002] argued that the moving arcs were consistent with the *Kullen* [2000] IMF rotation model. The mechanism for bending and multiple arcs was unclear.

[13] In this paper, we study arcs to differentiate between the various models that have been proposed. The main distinguishing feature that we will investigate is the time delay that is expected in any correlation between the IMF orientation and the local time at which arcs form.

### 3. Instrumentation and Survey

[14] In order to identify the arcs, we use auroral images from two of the Far Ultra Violet (FUV) cameras on the IMAGE spacecraft [*Mende et al.*, 2000a, 2000b, 2000c]. The cameras we use are the Wideband Imaging Camera (WIC) and the Spectrographic Imager 121.8 nm camera (SI12). WIC is sensitive to emissions in the spectral range 140–190 nm,

WIC: 27/12/2000 23:42UT

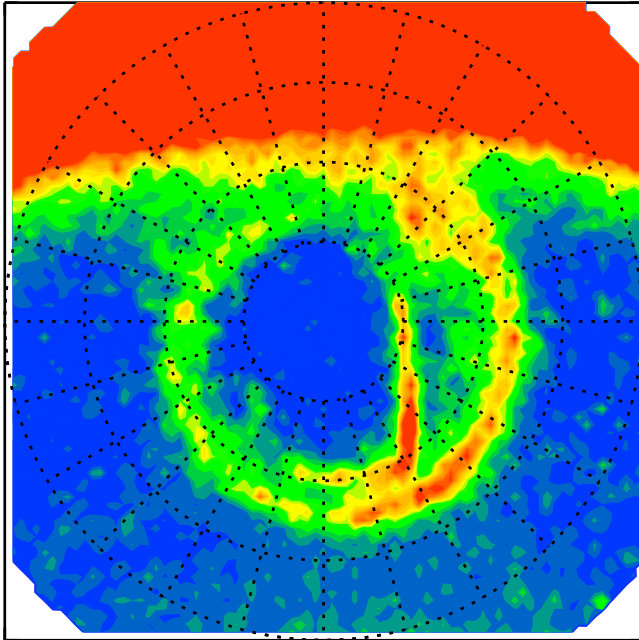


**Figure 2.** An example transpolar arc that was included in the survey, as observed 12 min after the arc first emerged into the polar cap. The image is projected onto a magnetic latitude/magnetic local time grid, with noon at the top of the image. Dayglow is visible at the top, the main auroral oval is at about  $65^{\circ}$ N magnetic latitude, and the arc has formed and extended into the polar cap. The arc first formed at 2 MLT.

and provides high spatial resolution images at 2 min cadence. (At apogee, a pixel in a WIC image corresponds to a  $52 \times 52$  km footprint.) The SI12 instrument is sensitive to a narrow band at 121.8 nm, which corresponds to the Doppler-shifted Lyman- $\alpha$  emission line, thus imaging proton-induced auroras. SI12 images are available at lower spatial resolution (at apogee, a pixel corresponds to a  $92 \times 92$  km footprint), but at the same temporal resolution as WIC. Due to the narrow sensitivity to Doppler-shifted emissions, the SI12 instrument is not sensitive to dayglow, unlike WIC.

[15] IMF data are taken from the OMNI high-resolution observatory data set, which combines solar wind data from a variety of sources which are lagged to the nose of the magnetopause as described by *King and Papitashvili* [2005]. We use 5 min averages of the IMF lagged to the magnetopause, from which we in turn calculate averages for various 1 h blocks before and after the time at which the observed transpolar arcs first emerged from the auroral oval (which is determined to a 2 min cadence).

[16] IMAGE observed the Northern Hemisphere aurora between 2000 and 2003, and the Southern Hemisphere aurora from 2003 to 2005. We examined both WIC and SI12 data between June 2000 and September 2005, and identified 131 transpolar arcs. In order to make our conclusions as generally applicable as possible, we applied as few criteria as necessary to ensure we had identified clear examples of transpolar arcs. We selected auroral arcs poleward of the main auroral oval which satisfied three criteria. First,

we required the emergence of the arc from the auroral oval to be observed by the WIC and/or SI12 instruments. The IMAGE spacecraft was in a 14.2 h orbit, and images were not available at perigee; any arcs which formed during the perigee data gap were not included as their start time could not be determined accurately. Secondly, we only included arcs which persisted for at least 30 min. Thirdly, we required the arc to make a significant protrusion into the polar cap at some point in its lifetime. (In other words, auroral emissions which were mainly oval-aligned for their entire lifetime were not included, although arcs which formed mainly along the oval but then moved into the polar cap were included.) An arc was not required to stretch across the entire polar cap to be selected (i.e., not all of the transpolar arcs in our survey form full thetas). Although we have not followed the subclassification system used by *Kullen et al.* [2002], we note that all four of their clear, individual arc types could satisfy our criteria. (*Kullen et al.* [2002] stated that their oval-aligned arcs do not move considerably but could be quite separated from the main oval; in such a case, this could count as a “significant protrusion”.) There were four examples in our data set which could be identified as bending arcs.

[17] An example arc is shown in Figure 2, as observed by the WIC camera a short while after its formation. The magnetic local time at which each arc first formed was identified in the earliest image after the arc’s first emergence in which it was possible to do so unambiguously (in this case, the arc formed at 2 MLT). A list of the start times of the arcs, the initial magnetic local time, the uncertainty in the initial magnetic local time and the hemisphere in which each arc was observed is included in the auxiliary material.<sup>1</sup>

#### 4. IMF Dependence

[18] Figure 3 shows a polar histogram of the IMF dependence of the transpolar arcs in this survey, normalized to the background IMF distribution between 2000 and 2005, then scaled such that the sum of the normalized distribution is 100%. The overwhelming majority of the events we identified occurred when the IMF (averaged over the preceding hour) was northward, consistent with previous results [e.g., *Berkey et al.*, 1976; *Kullen et al.*, 2002]. Of the 131 arcs, 112 occurred when the average IMF in the hour before the arc first emerged was northward, 8 occurred when it was southward, and no IMF data were available for the remaining 11 arcs. In four of the eight cases where the IMF was on average southward in the hour before the first emergence of the arc, the IMF was northward an hour prior to the arc forming, but turned southward between 30 and 45 min before the time identified as the start of the arc. Two of the other southward IMF arcs were events which would be identified as “bending arcs” by *Kullen et al.* [2002]: the arc initially forms aligned with the main auroral oval, and then “swings out” into the polar cap. The four bending arcs we identified occurred when the average clock angles over the hour preceding the start of the arc were  $+87^{\circ}$ ,  $+120^{\circ}$ ,  $-104^{\circ}$  and  $-74^{\circ}$ . This is consistent with the results of *Kullen et al.* [2002], who found 22 examples of bending arcs which were

<sup>1</sup>Auxiliary materials are available at <ftp://ftp.agu.org/apend/ja/2011ja017209>.

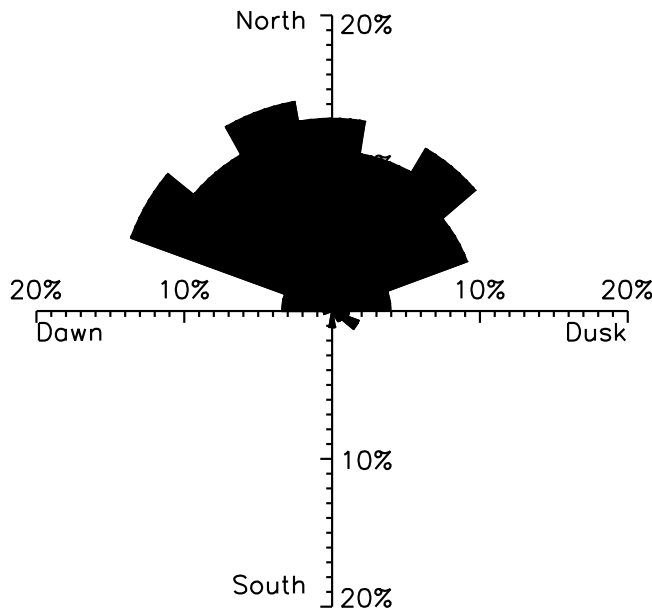


**Figure 3.** A histogram of the IMF clock angle dependence of the transpolar arcs identified in this survey. The radius of each wedge indicates that the number of arcs where the clock angle of the average IMF over the hour prior to start of the arc was in the corresponding clock angle bin, normalized to the background IMF distribution between 2000 and 2005, and scaled such that the total of all of the wedge radii is 100%.

equally likely to occur for northward as for southward IMF (evaluated over the hour prior to the start of the arc), and typically for  $B_Y$ -dominated IMF.

[19] Figure 4 shows a superposed epoch analysis of the IMF observed before and after the start time of each transpolar arc. Figure 4 shows (from top) the  $B_X$  and  $B_Y$  components, the magnitude of  $B_Y$ , the  $B_Z$  component and the total magnetic field. The blue line represents the Northern Hemisphere events, the red line represents Southern Hemisphere events, and the black line shows the combined data. No net sign in the  $B_X$  or  $B_Y$  component is evident, but  $B_Y$  has an average magnitude of 4 nT both before and after the start of the arc. Arcs in both hemispheres are associated with an increase in the  $B_Z$  component which starts on average about 3 h before the arc is first observed. The  $B_Z$  component decays after the start of the arc, but remains typically positive for about 5 h after the start of the arc.

[20] Figure 5 shows the IMF  $B_Y$  dependence of the magnetic local time at which the arcs first form. The panels show the results if  $B_Y$  is evaluated over a 1 h period at various times before the arc first forms (0–1, 1–2, 3–4, and 9–10 h before the arc start time). In each panel, the events which were observed in the Northern Hemisphere are indicated by black symbols, and the local time is indicated by the left-hand scale. The events which were observed in the Southern Hemisphere are plotted in red, with the local time indicated by the right-hand scale, which is reversed about midnight. Each point has an associated error bar, which indicates the uncertainty in determining the local time of the event. This was taken to be at least 0.5 h in magnetic local time,

but in some cases it was much larger. This was particularly the case for bending arcs and arcs which initially formed aligned with the auroral oval and subsequently moved into the polar cap: If the initial alignment is close to parallel to the oval, then the local time at which the arc first emerges into the polar cap is less clear. To quantify the dependence, each panel shows the correlation coefficient  $\rho$ . To take account of the evident reversed behavior in the Southern Hemisphere, the local times of the Southern Hemisphere arcs have been reversed about midnight; that is, the correlation coefficient is calculated according to the left-hand scale for MLT. Since the local time for Northern Hemisphere arcs decreases from 06 MLT, through 00 MLT toward 18 MLT as  $B_Y$  becomes increasingly positive, the correlation coefficient is negative. As it is not clear that any relationship between the initial local time and  $B_Y$  should be linear, we have calculated the Spearman's Rank correlation coefficient. In the top panel (representing the average  $B_Y$  components in the hour immediately before the arc

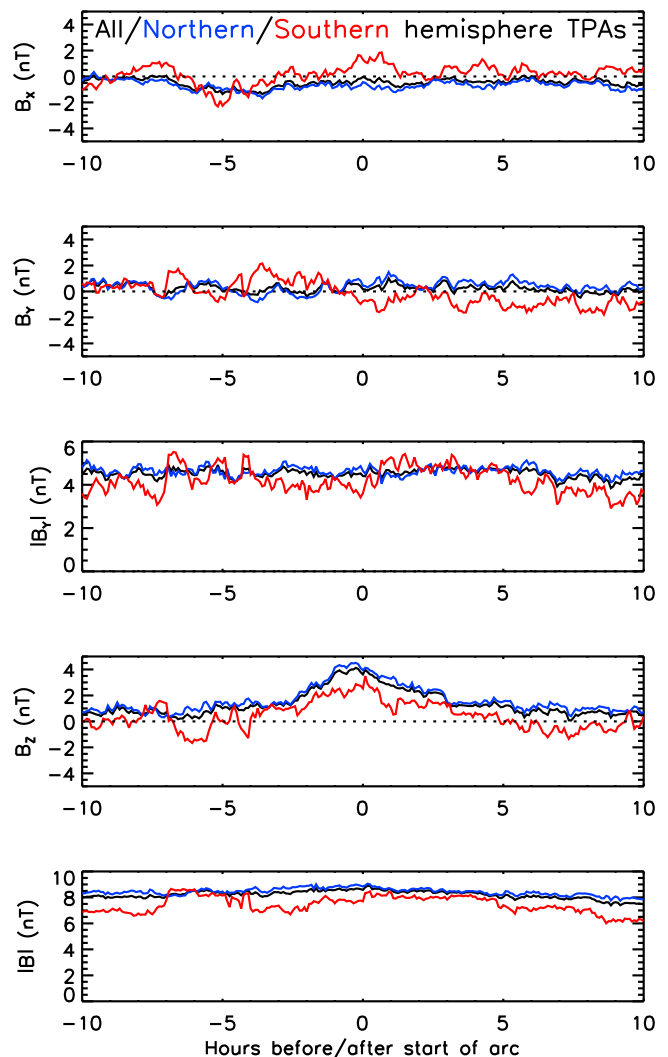


**Figure 4.** A superposed epoch analysis of the IMF components before and after the start time of the 131 transpolar arcs. The panels show, from top, the mean values of  $B_X$ ,  $B_Y$ ,  $|B_Y|$ ,  $B_Z$  and  $|B|$  before and after the start of the arc.

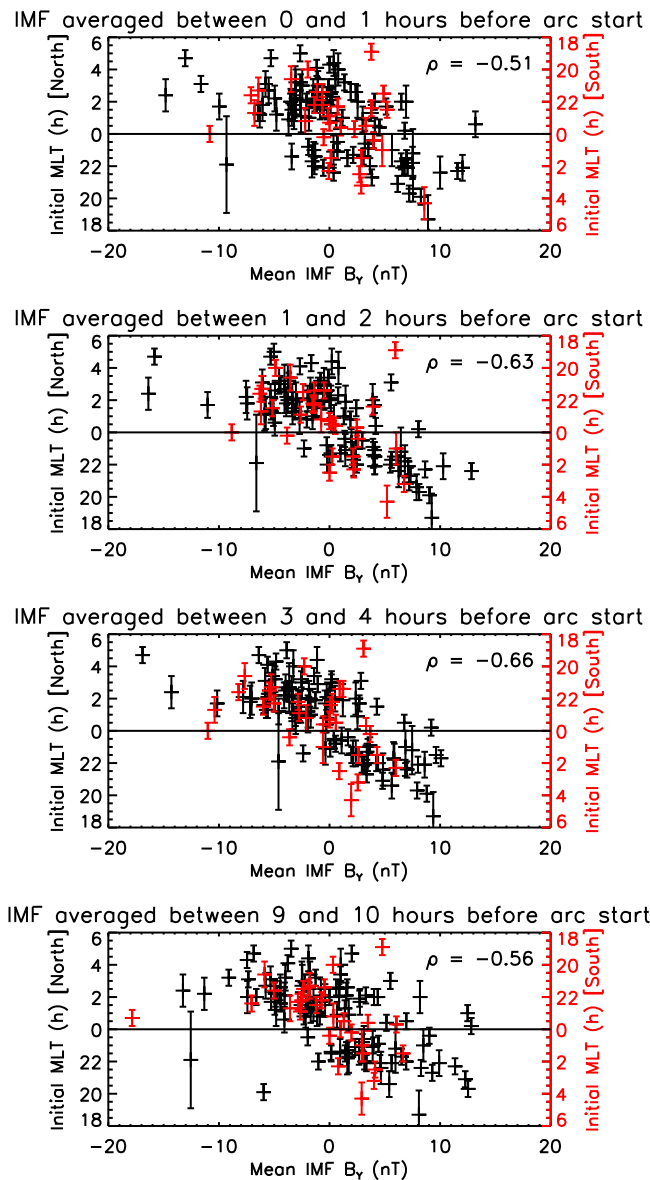


**Figure 5.** The dependence of the initial magnetic local time of the arcs in this study on the IMF  $B_Y$  component averaged over 1 h periods starting 1, 2, 4 and 10 h before the start of the arc. Each black point represents the initial magnetic local time and IMF  $B_Y$  component relating to an individual arc that was observed in the Northern Hemisphere (left-hand scale). The red points represent arcs that were observed in the Southern Hemisphere, and are plotted according to the right-hand scale, which is reversed about midnight. The uncertainty on each MLT is indicated by error bars.

start times), there is evidence for the trend reported by *Gussenhoven* [1982] and *Gusev and Troshichev* [1986]: when  $B_Y < 0$ , the arcs tend to form postmidnight in the Northern Hemisphere and premidnight in the south. When  $B_Y > 0$ , this trend is mostly reversed, although interestingly the scatter does not appear to be centered on the origin. The correlation coefficient is modest ( $\rho = -0.51$ ). However, when the  $B_Y$  component is averaged between 1 and 2 or between 3 and 4 h before the arc start time, the trend

becomes clearer and the correlation coefficient becomes larger in magnitude ( $\rho = -0.63$  and  $-0.66$ ). The trend is still present if the  $B_Y$  component is averaged between 9 and 10 h before the start of the arc, but the correlation is weaker. The same trend is observed if the initial local time is plotted against the IMF clock angle, rather than the  $B_Y$  component (not shown).

[21] Figure 6 shows the correlation coefficient,  $\rho$ , as a function of time relative to the start of the arc. Each data point represents the correlation coefficient based on a 1 h average of the  $B_Y$  component at a certain number of hours before or after the arc start time. The vertical dotted line at time zero indicates the start time. As is evident in Figure 5, the correlation with the  $B_Y$  component evaluated over the hour immediately preceding the start of the arc is relatively weak, and the correlation peaks if the hourly averaged  $B_Y$  component is evaluated between 3 and 4 h before the start of the arc. The horizontal dotted line at  $\rho = -0.2$  indicates the line below which a correlation coefficient is statistically significant at a 98% confidence level. The level at which  $\rho$  becomes significant is a factor of both the chosen confidence level and the number of events. (A correlation coefficient of 0.5 implies the same strength correlation regardless of the sample size, but it becomes more significant as the sample size increases: In other words, there is a smaller probability of the sample having a correlation coefficient of 0.5 if there is in fact no correlation at all in the population.) For negative correlation coefficients below this confidence level, the probability that the population correlation is really zero is less than 2%. In other words, values of  $\rho < -0.2$  are associated with p values of less than 2%.

[22] *Kullen et al.* [2002] observed an opposite tendency for their moving arcs from that observed for stationary arcs if the  $B_Y$  component was evaluated during the lifetime of the arc. To investigate whether this is the case in our data set, Figures 7 and 8 repeat the above analysis for the subset of arcs which were observed to move more than 2 h in magnetic local time between the arc first forming and the time at which either they fade away, or the IMAGE spacecraft ceases to observe them (e.g., due to a perigee data gap). 31 transpolar arcs moved either downward or duskward

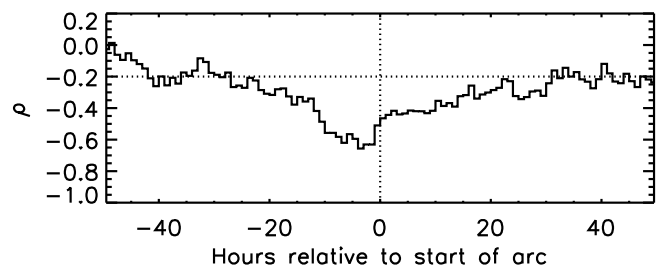


**Figure 6.** The Spearman's rank coefficient ( $\rho$ ) of the correlation between the initial MLT of all 131 arcs and the IMF  $B_Y$  component averaged over a 1 h period at varying times relative to the arc's first emergence into the polar cap. The vertical dotted line indicates the arc's start time, and the horizontal dotted line indicates the correlation coefficient below which the null hypothesis that the initial MLT and IMF  $B_Y$  component are uncorrelated ( $\rho = 0$ ) is rejected with 98% confidence.

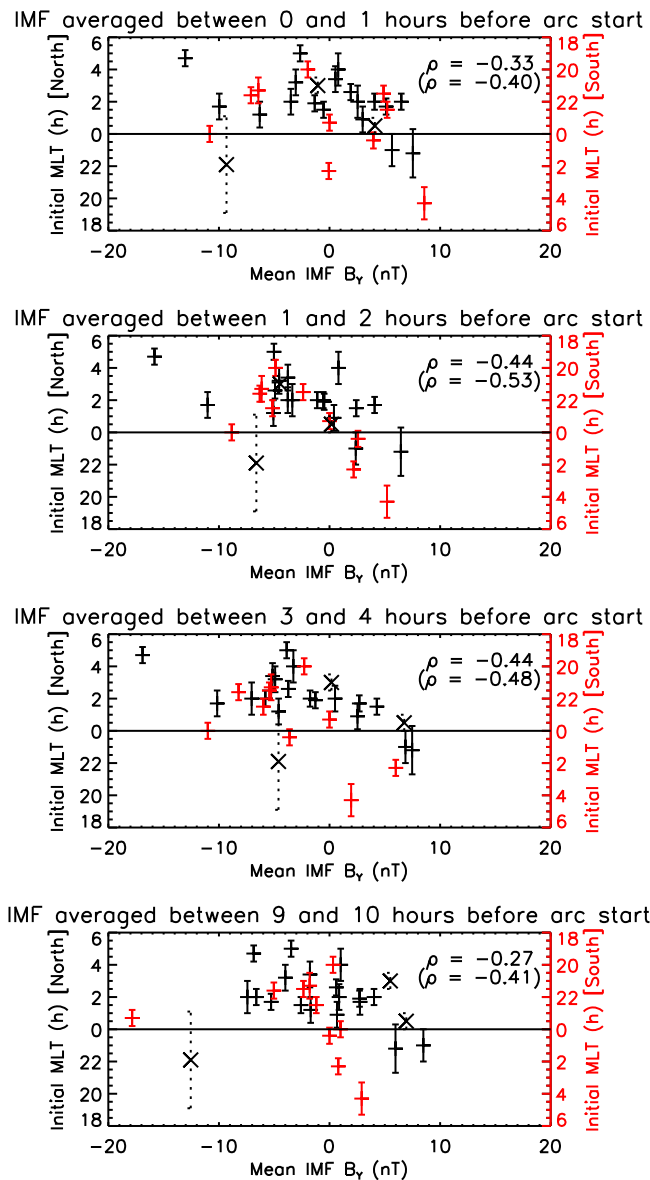


**Figure 7.** Same as Figure 5 but only for the 31 arcs that move more than 2 h of MLT during the lifetime of the event. The top correlation coefficient in each panel refers to all moving arcs. “Bending” arcs are indicated by dotted error bars and crosses, and the correlation coefficients indicated in brackets are for nonbending (but moving) arcs only.

by more than 2 h of MLT. The same trend is present when considering the  $B_Y$  component before the arc formed, although the correlation coefficients are weaker than in the sample of all 131 TPAs. As the sample is smaller, the critical value at which  $\rho$  becomes significant at 98% confidence becomes larger in magnitude ( $\rho = -0.42$ ). The correlation coefficient is therefore not statistically significant if  $B_Y$  is evaluated over the hour immediately preceding the first emergence of the arc ( $\rho = -0.33$ ), but it is significant if  $B_Y$  is averaged over 1 h between 1 and 4 h before the start time of the arc. If a reversal in  $B_Y$  is required to trigger a moving arc, then given the negative correlation coefficients preceding the arc start time, we would expect to see a positive coefficients

if  $B_Y$  is evaluated over the hour or two immediately following the start time of the arc. In fact, we find that the data are uncorrelated if  $B_Y$  is evaluated after the start time (Figure 8). The fact that the negative correlation is no longer present after the start time demonstrates that although the moving arcs are not generally associated with a reversal in the sign of  $B_Y$ , they do occur at times when the  $B_Y$  component changes (although not necessarily by much, and the change could be an increase in magnitude).

[23] To check the lack of a link with a sign reversal, we also plotted the lagged IMF data from 2 h before the start time until the time at which the arc disappeared from view (or the observations ceased) for each of the 31 arcs which moved by more than 2 h in MLT (Figure 9). We identified whether the  $B_Y$  component between 2 h and 1 h before the start of the arc was generally positive or generally negative, and whether  $B_Y$  during the lifetime of the arc was generally positive or generally negative. Following the method used by *Kullen et al.* [2002], an arc was defined to be associated with a reversal in  $B_Y$  if the sign of  $B_Y$  changed in the hour preceding the start of the arc or in the first 10 min of its life (to account for uncertainty in the lag applied to the IMF data) from a generally positive orientation beforehand to a generally negative orientation during the arc’s lifetime (or vice versa). Only 8 arcs were associated with a  $B_Y$  sign change (TPAs 8, 13, 15, 19, 63, 70, 119, and 127 in Figure 9) and the IMF data from one event (TPA 126) were unclear due to a data gap.

[24] As noted earlier in this section, our event list includes four “bending” arcs, two of which occur when the lagged IMF over the hour prior to the start of the arc is northward, and two which occur when the IMF is southward (but with a strong  $B_Y$  component in all four cases). The nightside connection point of three of these arcs moves by more than 2 h of magnetic local time, and so they are included in Figures 7 and 8. They are indicated in Figure 7 by points with dotted error bars. Two of the bending arcs appear to follow the main trend, but the third is a distinct outlier albeit with a large error bar due to the complex nature of its formation. Within this error bar, it might be placed on the edge of the main distribution, but if the three bending arcs are removed then the correlation coefficients in brackets in Figure 7 are obtained. These correlations are plotted in Figure 10; they are stronger, peaking in magnitude at about  $-0.6$  if the IMF is evaluated between 6 and 7 h before the start of the arc, and it is statistically significant (at 98% confidence) for most 1 h blocks between 1 and 2 h and 8 and 9 h before the start time of the arc.

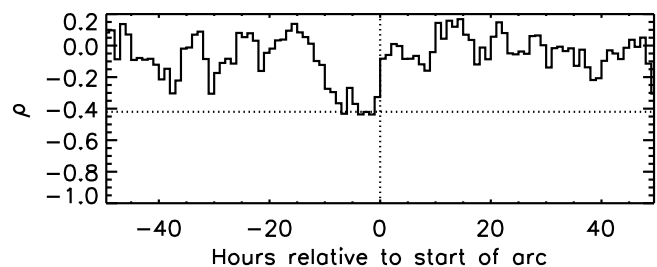


**Figure 8.** Same as Figure 6 but only for the 31 arcs that move more than 2 h of MLT during the lifetime of the event.

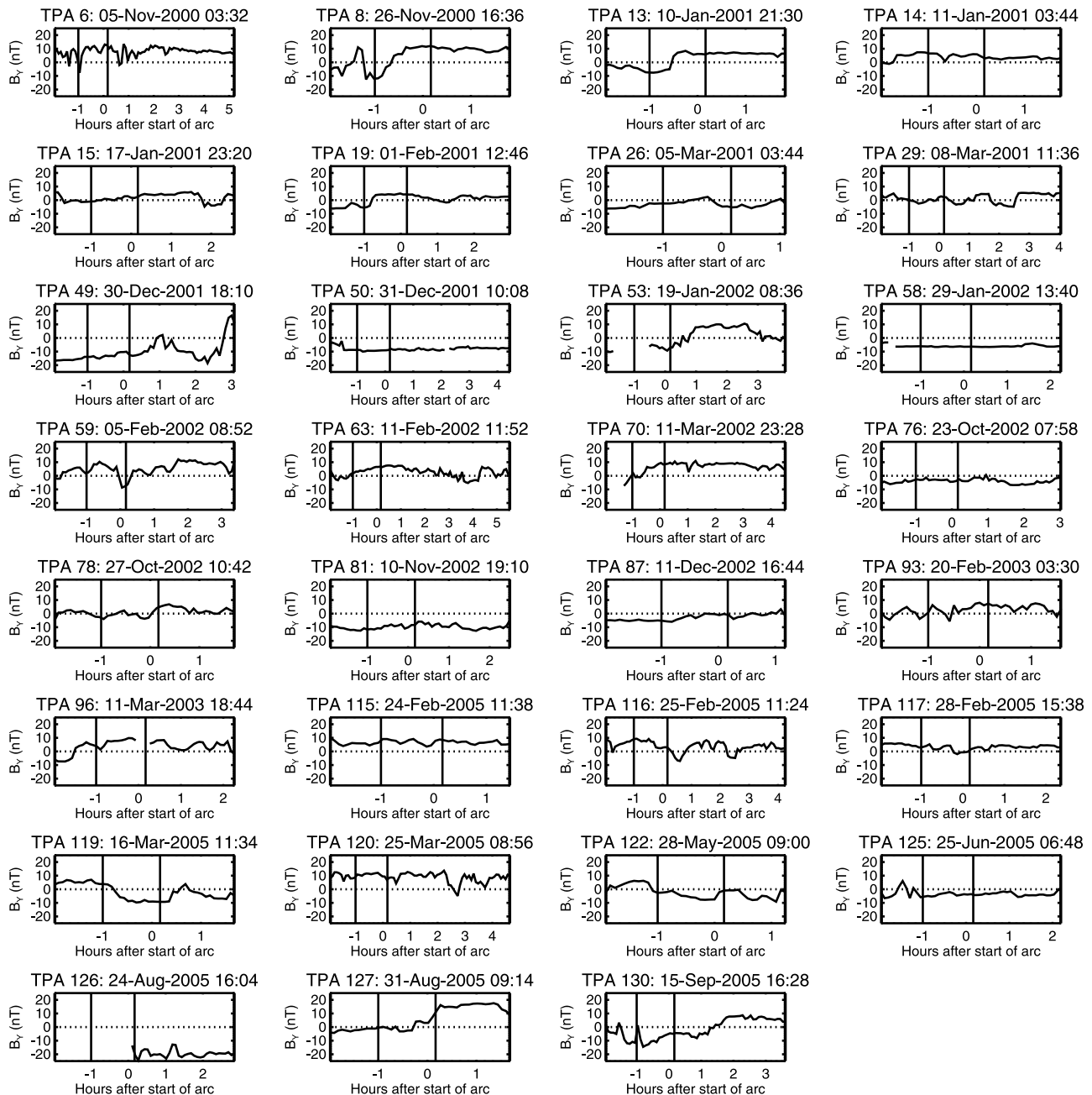


**Figure 9.** The IMF  $B_Y$  component as a function of time relative to the first emergence of each arc that subsequently moved more than 2 h in magnetic local time. The data are plotted from 2 h before the arc first emerged until the arc either faded away or ceased to be observed by IMAGE (e.g., due to a data gap). The vertical lines are placed 1 h before and 10 min after the arc emerged, bracketing the intervals in which *Kullen et al.* [2002] observed magnetic field reversals.

[25] In Figures 11 and 12, we have shown the correlation between the IMF  $B_Y$  component and the initial local time of the 100 transpolar arcs which did not move in their observed lifetime, or moved by less than 2 h of MLT. Since this subset forms about three quarters of our entire sample, the behavior is similar to that observed in Figures 5 and 6. However, the correlation before the arc start time is stronger, and the peak in the correlation 3–4 h before the arc start time is more distinct. The strong correlation persists for several

hours after the start time, indicating that arcs with relatively little motion are associated with periods with a steady IMF  $B_Y$  component.

[26] *Reiff and Burch* [1985] predicted that there should also be a  $B_X$  dependence. They predicted that when  $B_Y$  is positive, arcs should initially form premidnight in both hemispheres when  $B_X < 0$  and postmidnight when  $B_X > 0$ , and that the opposite  $B_X$  dependence should occur when  $B_Y$  is negative. In Figure 13, we show the  $B_X$  dependence

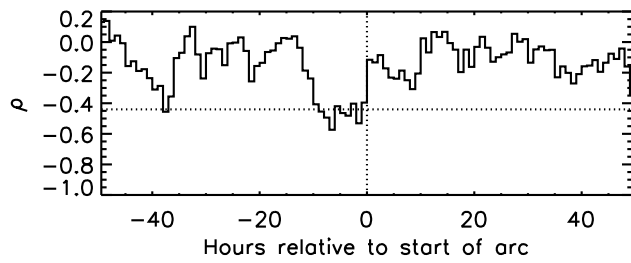


**Figure 10.** Same as Figure 8 but with the three arcs that could be classified as bending arcs (and where the nightside connection point moves more than 2 h of MLT) removed.

for various hourly intervals before the start of each arc. Figure 13 takes a similar form to Figure 5, with Northern Hemisphere arcs being indicated in black and Southern Hemisphere arcs being indicated in red. However, the

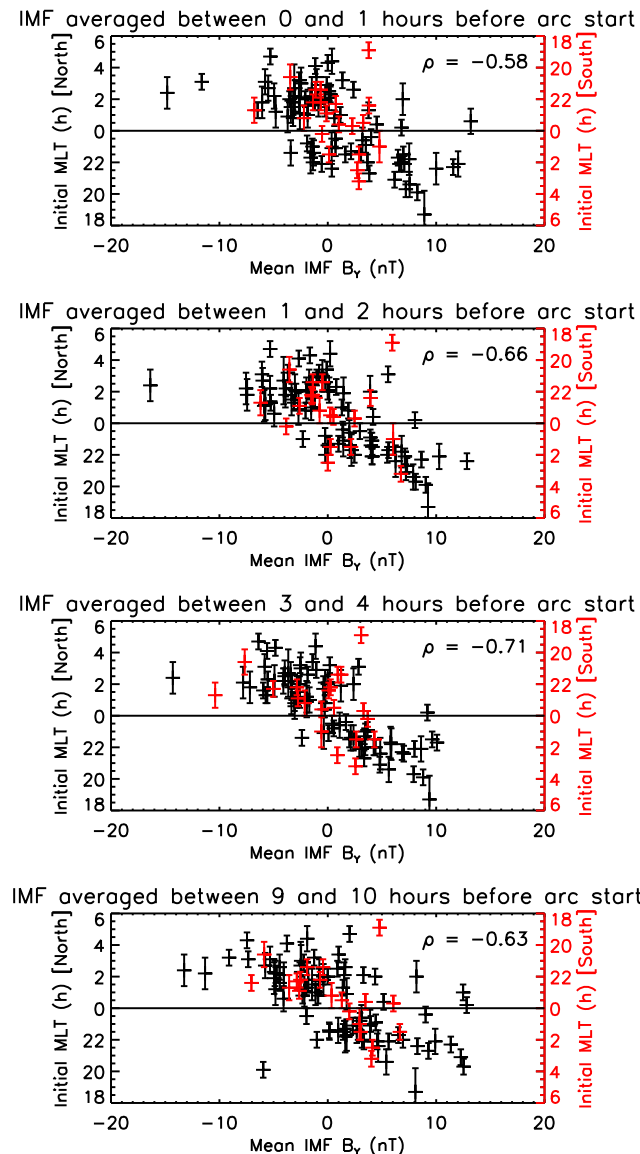


**Figure 11.** Same as Figure 5 but only for the 100 arcs without significant motion over the lifetime of the event.

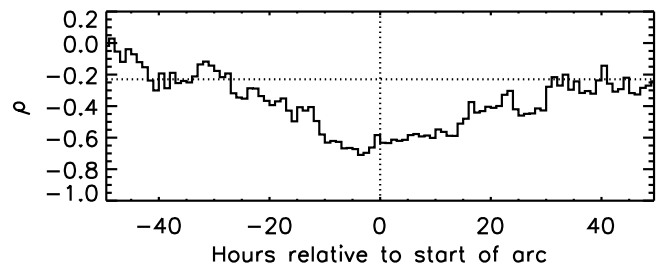


**Figure 12.** Same as Figure 6 but only for the 100 arcs without significant motion over the lifetime of the event.

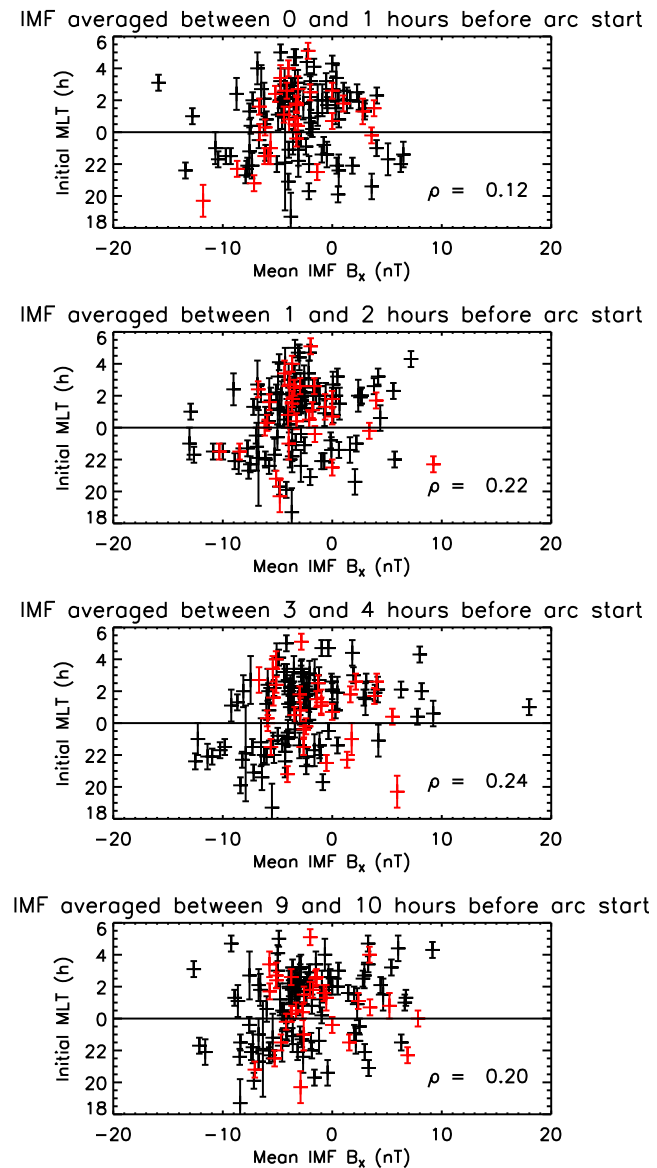


**Figure 13.** The dependence of the initial magnetic local time on the IMF  $B_x$  component prior to the initial emergence of the arc for all 131 arcs in the study. All arc local times are plotted according to the left-hand scale. The  $B_x$  components have been multiplied by  $-1$  for all events which occurred when the  $B_y$  component was negative, to reflect the prediction made by *Reiff and Burch* [1985].

horizontal axis represents hourly averages of the  $B_X$  component, and all points are plotted according to the MLT scale on the left-hand axis. The  $B_X$  components have been multiplied by  $-1$  for arcs which occurred when the hourly average  $B_Y$  component was negative. If the *Reiff and Burch* [1985] prediction is correct then a positive correlation should be observed, but there is no significant correlation.

## 5. Discussion

[27] In this paper, we have presented evidence for a correlation between the IMF  $B_Y$  component and the magnetic local time at which transpolar arcs form. In the Northern Hemisphere, arcs form predominantly pre-midnight when  $B_Y > 0$  and post-midnight when  $B_Y < 0$  (consistent with results reported by *Gussenhoven* [1982], and for oval-aligned transpolar arcs reported by *Kullen et al.* [2002]). The opposite relationship is observed in the Southern Hemisphere, as reported by *Gusev and Troshichev* [1986]. However, these correlations are strongest if the IMF is averaged 3–4 h prior to the first emergence of the arc. This delay is consistent with the typical time scale that can be deduced from the results of *Dungey* [1965], *Borovsky et al.* [1993], and *Milan et al.* [2007] for the passage of a newly opened magnetic field line from the dayside magnetopause and sunward edge of the polar cap to the point at which it is reclosed on the nightside at the plasma sheet and the nightside edge of the polar cap. This is indicative of a nightside driver for the formation of transpolar arcs, and is consistent with the observations that all of the arcs initially formed on the night side (all MLTs in Figure 5 are in the range  $18 < \text{MLT} < 06$ ). The delay required to affect magnetotail behavior is also consistent with the observation by *Milan et al.* [2010] that a significant correlation exists between the local time at which a substorm onset occurs and the IMF  $B_Y$  component, but that  $B_Y$  must have a positive or negative bias for several hours prior to substorm onset in order to influence the onset MLT. To our knowledge, all previous studies investigating the local time at which polar cap arcs are observed have investigated the effect of the IMF within the 2 h immediately prior to the first observation of the arc (and only *Gussenhoven* [1982] has examined the IMF more than 1 h in advance).

[28] We propose that the correlation between the local time at which the arcs form and the IMF  $B_Y$  component over the hour immediately preceding the arc is not a direct indicator of the physics involved in the formation of transpolar arcs, but it is a result of the finite time scale on which  $B_Y$  typically changes. Transpolar arcs without significant motion following their formation are well correlated with the IMF  $B_Y$  component for several hours after the arcs first form. This correlation shows that such arcs are associated with intervals where the IMF  $B_Y$  component is steady. On the other hand, the correlation between the initial local time of arcs which subsequently move by more than 2 h of magnetic local time and the mean  $B_Y$  component in the hour prior to their first appearance is weaker, and is not significant at the 98% confidence level. This indicates that moving arcs are associated with a changing IMF  $B_Y$  component. However, we did not find any evidence for moving arcs being triggered by a change in the sign of  $B_Y$ ; only 8 of the 31 arcs with significant motion and for which good IMF data were available were associated with a  $B_Y$  reversal from a generally

positive orientation more than 1 h beforehand to a generally negative orientation during the lifetime of the arc, or vice versa. Therefore, we eliminate mechanisms based on a sign change in  $B_Y$  as a general cause for either moving or stationary transpolar arcs [*Chang et al.*, 1998; *Kullen*, 2000]. The transpolar arcs in our survey are related generally to a period of northward IMF both before and after the start time (Figure 4). Therefore, in general the arcs in our survey are not triggered by a southward turning in the  $B_Z$  component as proposed by *Newell and Meng* [1995].

[29] The profile of the correlation that is observed between the local time at which moving arcs form and the IMF  $B_Y$  component more than 1 h beforehand is similar to that which is observed for stationary arcs. This is suggestive of a single mechanism for the formation of moving and stationary arcs which depends upon the orientation of the IMF more than 1 h before the arc is first observed, and a separate mechanism for their motion. The time delay in the correlation between  $B_Y$  and the local time of the arc is indicative of a mechanism where the formation of transpolar arcs is driven by plasma sheet dynamics, where the flux adjacent to the plasma sheet has a  $B_Y$  component which is determined by the IMF  $B_Y$  component several hours beforehand. This is in turn compatible with the observations that the plasma precipitation above transpolar arcs is similar to that observed above the poleward edge of the main oval, and is consistent with a plasma sheet source [e.g., *Peterson and Shelley*, 1984; *Frank et al.*, 1986]. Mechanisms which attribute the control of transpolar arc formation to the magnetopause (e.g., a direct link between reverse convection cells and transpolar arcs) would produce a stronger correlation between  $B_Y$  in the hour or so before the arc first forms. We therefore believe that mechanisms which link the formation of transpolar arcs to reverse convection patterns driven by reconnection between the IMF and the lobe [e.g., *Chiu et al.*, 1985; *Lyons*, 1985; *Sojka et al.*, 1994] are inconsistent with our observations.

[30] Of the mechanisms listed in Table 1 that do not invoke a  $B_Y$  sign change, one would expect a delayed correlation with the IMF  $B_Y$  component in the models proposed by *Reiff and Burch* [1985], *Makita et al.* [1991], *Rezhenov* [1995], and *Milan et al.* [2005]. However, the *Reiff and Burch* [1985] model predicts that the  $B_Y$  dependence should be opposite for positive and negative values of  $B_X$ . If this were the case, it would obfuscate a correlation in Figures 5, 7, and 11, and a correlation would be present in Figure 13.

[31] We are therefore left with the conclusion that the only models which can explain the formation of transpolar arcs are a combination of the two models proposed by *Makita et al.* [1991] and *Rezhenov* [1995], as concluded by *Kullen et al.* [2002], or the model proposed by *Milan et al.* [2005]. As noted by *Kullen et al.* [2002], neither of the former two models can explain the presence of moving transpolar arcs. Furthermore, in Figures 5, 7 and 11 there is a continuous distribution of arcs occurring between 20 and 04 MLT, suggesting that there is no clear division between arcs formed near the dawn or dusk oval and those formed in the midnight sector. Consequently, we believe that the *Milan et al.* [2005] mechanism is more likely, since through a single framework it explains the delay in the correlation between the IMF  $B_Y$  component and the local time at which

arcs form, the formation of stationary and moving arcs and the formation of arcs at all local times. The *Milan et al.* [2005] mechanism predicts that fast ionospheric flows should be observed coincident with the main auroral oval (i.e., on newly closed magnetic field lines) between the local time at which the arc forms and local midnight. This has been reported in a subsequent case study [*Goudarzi et al.*, 2008], but we plan to test this prediction on a larger number of events in a future paper.

[32] The *Milan et al.* [2005] mechanism also provides an explanation of why the correlation between the IMF  $B_Y$  component and the local time at which the arcs form remains strong after the initial emergence of arcs with little subsequent motion, but deteriorates rapidly in the hour before the arc start time for arcs which subsequently do move. In their mechanism, the motion of the arc is driven by the “stirring” of lobe flux as a result of reconnection between the IMF and the lobe. Lobe reconnection causes open flux to circulate within the polar cap, causing one or two flow cells depending upon the magnitude of the  $B_Y$  component [*Reiff and Burch*, 1985]. *Milan et al.* [2005] proposed that if an arc were situated on a lobe circulation cell, it would be carried in the direction of flow of that cell. *Milan et al.* [2005, Figure 9] provided an example sketch of the motion expected for an arc that had formed postmidnight in the Northern Hemisphere due to a negative  $B_Y$  beforehand but where the  $B_Y$  component had subsequently reversed. In this scenario, single lobe reconnection was occurring with a merging gap (the footprint of the field lines threading the reconnection site) located duskward of the arc. The arc was therefore located in the clockwise-convecting dawn cell, and so the arc was swept duskward. If  $|B_Y| < B_Z$  [*Milan et al.*, 2005, Figure 9a], then the motion continues as far as the boundary between the dawn and dusk cells. If  $|B_Y| > B_Z$  [*Milan et al.*, 2005, Figure 9b], then a single cell dominates and the motion can continue to the edge of the polar cap. In Figure 14a we have sketched what we predict to be the situation if the  $B_Y$  component remains steady between the time at which the outermost plasma sheet magnetic field line was first opened on the dayside (several hours before the arc first emerges) and the demise of the arc. In Figure 14b, we sketch the situation if  $B_Y$  increases in magnitude during this interval but does not change sign. Figure 14 follows a similar format to Figure 9 of *Milan et al.* [2005]; the thick black line denotes the open-closed boundary in the Northern Hemisphere, which is the edge of the polar cap. A transpolar arc, formed postmidnight due to the negative  $B_Y$  component, protrudes into the polar cap. The merging gap is indicated by a dotted line, and thin arrowed lines indicate the lobe convection cells which are excited. In the steady  $B_Y$  case (Figure 14a), we propose that the merging gap will be located near the arc, and so the arc will be situated near the boundary between the dusk and dawn lobe cells. Consequently, the subsequent motion of the arc will be limited (although the flow of field lines just antisunward of the merging gap might help the arc to grow into the polar cap). If, however, the IMF  $B_Y$  component increases in magnitude without changing sign (Figure 14b) then the merging gap will be located dawnward of the arc. Consequently, the arc will be embedded within the dusk circulation cell. Therefore, the arc will move dawnward. (If  $|B_Y| > B_Z$  then the dawn cell, indicated by a dotted arrowed line, may be totally absent

[*Reiff and Burch*, 1985].) In summary, motion of a transpolar arc from one side of the polar cap across the midnight sector to the far side requires a change in the sign of  $B_Y$  either before or after the initial emergence of the arc (as sketched by *Milan et al.* [2005, Figure 9]), but motion away from the midnight sector can be provided by an increase in the magnitude of the  $B_Y$  component without it changing sign (Figure 14). Since the motion of the arc is driven by the very recent history of the IMF, and the initial location is driven by the orientation of the IMF several hours beforehand, when the first field line which subsequently gives rise to the arc was initially opened on the dayside, the change in  $B_Y$  can occur at any point in time between the initial dayside opening of the field line (approximately 4 h before the first emergence of the arc) and the final demise of the arc.

[33] The correlation between the IMF  $B_Y$  component 3–4 h before the arc start time and the initial magnetic local time of the arc is weaker for the arcs which move more than 2 h in magnetic local time compared with those arcs which move less than 2 h. However, the correlation is still significant at a 98% confidence level: In other words, the probability of obtaining the observed correlation coefficient ( $\rho = -0.44$ ) if there is in fact no correlation in the population is less than 2%. If the local time at which an arc forms is indeed driven by the  $B_Y$  component at the boundary between the plasma sheet and the lobe, then the IMF which determines that  $B_Y$  component will be observed at a slightly different number of hours before the arc first emerges in each case. The calculations given above for the time taken for a newly opened magnetic field line to reach the plasma sheet give typical time scales, but in practice there will be variation due to variation in the solar wind speed, the size of the polar cap and lobe (affecting the distance which a magnetic field line has to travel) and the bursty nature of reconnection in the magnetotail. A lobe field line with a given  $B_Y$  component may arrive at the boundary with the plasma sheet after, say, 3 h, but it will only affect the location of the arc when reconnection occurs in the magnetotail, which may be a while later. Therefore, we expect some “smearing” in the distributions in Figures 5, 7, and 11. This is particularly the case for moving arcs, since these are evidently associated with periods where the IMF  $B_Y$  component is changing.

[34] We have tried to avoid splitting our events into different morphological types where this has not been necessary. However, we do note that our event list includes four arcs which could be classified as “bending” arcs (hook-shaped features which form with both ends attached to the main oval, with one end remaining fixed and the other swinging out into the polar cap) which all formed when the IMF is dominated by its  $B_Y$  component as reported by *Kullen et al.* [2002]. Two of these bending arcs formed when the IMF had a northward component and two when the IMF had a southward component (also reported by *Kullen et al.* [2002]). It is not possible to determine on the basis of four events whether or not these are formed by the same mechanism as the other arcs. Three of the bending arcs are classified as having significant motion, two of which fall within the typical MLT/ $B_Y$  distribution in Figure 7. The third is a distinct outlier, but is associated with a large uncertainty in its initial local time. Since there are only 31 arcs with significant motion, removing the three bending arcs does

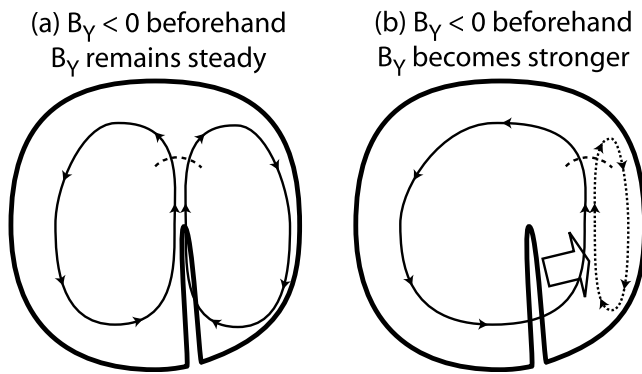


**Figure 14.** The expected polar cap convection patterns following the formation of a postmidnight transpolar arc in the Northern Hemisphere, when  $B_Y$  is moderately positive. The thick black line denotes the open-closed boundary, encircling the polar cap and with a transpolar arc protruding into the polar cap. Noon is located at the top, midnight is located at the bottom, dusk and dawn are located on the left and right of each panel. The merging gap (the footprint of a reconnection site between the IMF and lobe magnetic field lines) is indicated by a short dotted line, and the ionospheric flows, which are excited by lobe reconnection, are indicated by thin arrowed lines. (a) The situation if the  $B_Y$  component remains reasonably steady: the merging gap and boundary between the two lobe cells are located near the arc, and so the arc's scope for motion is limited. (b) The situation if the  $B_Y$  component becomes stronger but remains negative: the merging gap is located downward of the arc, and so the arc is dragged downward by the flows in the dawn cell, as indicated by the large arrow.

improve the correlation coefficient somewhat, but it is not clear whether this is because they are truly formed by a different mechanism or whether it is simply due to the poor determination of the initial local time of the outlying arc.

[35] It is possible that the reason that *Kullen et al.* [2002] came to the conclusion that moving arcs are triggered by a change in the  $B_Y$  component might be due to their definition of a moving arc. These were defined as “arcs which moved across the entire polar cap unless they fade before reaching the other side of the oval”. For an arc to cross the midnight sector and reach the far side of the oval does require a  $B_Y$  sign change either before or during the lifetime of the arc. Therefore, by requiring the direction of motion to be toward the far side of the polar cap, it is possible that the  $B_Y$  change required for motion might be concluded to be a trigger, particularly if there is uncertainty in the propagation time of the IMF to the magnetopause. In examining moving arcs, we consider arcs with less substantial motion that *Kullen et al.* [2002] might have classified as “midnight arcs” (which they noted often moved toward one side of the oval) as well as arcs with motion away from the noon/midnight meridian.

[36] All of the discussion above has implied that transpolar arcs occur simultaneously in both hemispheres, at opposite sides of the noon/midnight meridian. However, *Østgaard et al.* [2003] presented two intervals with simultaneous Northern and Southern Hemisphere observations available, and in both cases an arc was only observed in the hemisphere in which it was winter. If their observations were

to be interpreted in the context of the *Milan et al.* [2005] model, then we would suggest that in both intervals, transpolar arcs had formed in both hemispheres, but that the arc in one hemisphere had then moved from its original location toward the edge of the polar cap, becoming indistinguishable from the main auroral oval by the time the polar cap was first observed in that hemisphere. This is possible because the subsequent motion of an arc in the *Milan et al.* [2005] model is driven by lobe reconnection, which can occur at different rates in the two hemispheres (or even just in one hemisphere). This explanation would require lobe reconnection to occur preferentially in the summer hemisphere (in which no TPA was observed) in both cases. This preference would be consistent with observations that lobe reconnection is predominantly a summer hemisphere effect [*Crooker and Rich*, 1993; *Lavraud et al.*, 2005]. In the first case presented by *Østgaard et al.* [2003], no data were available in the Southern (summer) Hemisphere for the first 75 min of the Northern Hemisphere arc's lifetime, which would allow enough time for the arc to move to the edge of the oval. In the second case, the arc was observed in the first available image, so the initial formation time could not be determined.

## 6. Conclusions

[37] In this paper, we have provided evidence for the following observational features of transpolar arcs:

[38] 1. A correlation is observed between the IMF  $B_Y$  component and the magnetic local time at which transpolar arcs form.

[39] 2. The peak correlation occurs if the IMF  $B_Y$  component is evaluated 3–4 h before the start of the arc, consistent with expected time scales for flux transport from the dayside magnetosphere to the magnetotail plasma sheet and therefore indicative of a formation mechanism based on magnetotail processes. The correlation is weaker if  $B_Y$  is evaluated over the hour immediately before the arc, indicating that the formation is not driven by magnetopause processes such as lobe reconnection.

[40] 3. In the Northern Hemisphere, arcs form preferentially postmidnight when  $B_Y < 0$  and premidnight when  $B_Y > 0$ , as observed by *Gussenhoven* [1982].

[41] 4. The opposite trend is present in the Southern Hemisphere, also reported by *Gusev and Troshichev* [1986].

[42] 5. There is no clear divide between arcs which form on the dawn or dusk side of the oval and those which form near midnight, indicative of a common formation process regardless of the location at which the arc forms.

[43] 6. The ~4 h peak occurs for both stationary and moving arcs, indicating a common formation process for moving and stationary arcs.

[44] 7. For stationary arcs, the correlation remains strong for several hours after the start of the arc, indicating that arcs are stationary if they form during intervals of steady IMF  $B_Y$ .

[45] 8. For moving arcs, the relationship between  $B_Y$  and MLT is uncorrelated in the hour prior to the formation of the arc and during the arc's lifetime. This indicates that the motion of transpolar arcs is associated with intervals where the IMF  $B_Y$  component changes.

[46] 9. We emphasize that, contrary to the predictions of some models and conclusions of some previous observational studies, there is no statistical evidence for a  $B_Y$  or  $B_Z$

**Table 2.** A Summary of the Comparison in Section 5 Between the Predictions of the Models Listed in Table 1 and the Observations Presented in This Paper

Model	Consistent With Observations?
Chiu <i>et al.</i> [1985]	No. Predicts correlation between $B_Y$ and initial arc MLT should peak immediately before formation of arc (not observed in Figures 6, 8, or 12).
Lyons [1985]	No. Predicts correlation between $B_Y$ and initial arc MLT should peak immediately before formation of arc (not observed in Figures 6, 8, or 12).
Reiff and Burch [1985]	No. Predicts an MLT dependence on $B_X$ (not observed in Figure 13).
Makita <i>et al.</i> [1991]	No. Cannot explain arcs away from dawn/dusk side of oval or moving arcs (arcs are observed at all nightside MLTs in Figure 5).
Sojka <i>et al.</i> [1994]	No. Predicts correlation between $B_Y$ and initial arc MLT should peak immediately before formation of arc (not observed in Figures 6, 8, or 12).
Newell and Meng [1995]	No. Requires $B_Z$ sign change trigger (not observed in Figure 4).
Rezhnev [1995]	No. Cannot explain observation that changing $B_Y$ conditions cause motion of arcs (Figure 8).
Chang <i>et al.</i> [1998]	No. Requires $B_Y$ or $B_Z$ sign change trigger (not observed in Figures 6, 8, or 12 [ $B_Y$ ] or Figure 4 [ $B_Z$ ]).
Kullen [2000]	No. Requires $B_Y$ sign change trigger (not observed in Figures 6, 8, or 12).
Milan <i>et al.</i> [2005]	Yes. Explains MLT/ $B_Y$ dependence in both hemispheres (Figure 5), formation of arcs at all nightside MLTs (Figure 5) and formation of both moving and stationary arcs (Figures 7 and 11).

sign change “trigger” for the formation of transpolar arcs.  $B_Y$  changes discussed above may be small, and may consist of an increase in magnitude (rather than a reversal). Increases, decreases or sign changes in the  $B_Y$  component only affect the motion of the arc, not its formation.

[47] A summary of the comparison between the various model predictions and the observations summarized above is given in Table 2. The sense of the correlation and the requirement for several hours’ delay in the IMF data is consistent with the mechanism proposed by Milan *et al.* [2005], whereby the location at which arcs form is determined by the cross-tail component of the magnetic field in the part of the lobe that is immediately adjacent to the plasma sheet. This cross-tail component is in turn determined by the IMF  $B_Y$  component several hours beforehand [Cowley, 1981]. The observation that arcs which subsequently have little motion are associated with intervals where the IMF  $B_Y$  component is steady, but arcs which move are associated with intervals where  $B_Y$  changes (but not necessarily reversing in sign, and not necessarily changing by much) is also consistent with the Milan *et al.* [2005] mechanism, which ascribes the motion of an arc to IMF  $B_Y$  component that is observed after the arc forms.

[48] **Acknowledgments.** The authors were supported by STFC rolling grant ST/H002480/1. The IMAGE FUV data were provided by the NASA Space Science Data Center (NSSDC), and we gratefully acknowledge the PI of FUV and S. B. Mende of the University of California, Berkeley. The OMNI IMF data were obtained through the

NASA Goddard Space Flight Center Coordinated Data Analysis Web (CDAWeb). We are grateful to J. H. King and N. Papatashvili for provision of the OMNI data, as well as to the PIs of the magnetic field and plasma instruments on the IMP-8, Wind, Geotail and ACE spacecraft, whose data contributed to the OMNI data set for the time span investigated in this study. We are also grateful to the referees for their comments.

[49] Philippa Browning thanks the reviewers for their assistance in evaluating this paper.

## References

- Berkey, F. T., L. L. Cogger, S. Ismail, and Y. Kamide (1976), Evidence for a correlation between Sun-aligned arcs and the interplanetary magnetic field direction, *Geophys. Res. Lett.*, *3*(3), 145–147, doi:10.1029/GL003i003p00145.
- Borovsky, J. E., R. J. Nemzek, and R. D. Belian (1993), The occurrence rate of magnetospheric-substorm onsets: Random and periodic substorms, *J. Geophys. Res.*, *98*(A3), 3807–3813, doi:10.1029/92JA02556.
- Boudouridis, A., E. Zesta, L. R. Lyons, P. C. Anderson, and D. Lummerzheim (2003), Effect of solar wind pressure pulses on the size and strength of the auroral oval, *J. Geophys. Res.*, *108*(A4), 8012, doi:10.1029/2002JA009373.
- Burke, W. J., M. S. Gussenhoven, M. C. Kelley, D. A. Hardy, and F. J. Rich (1982), Electric and magnetic field characteristics of discrete arcs in the polar cap, *J. Geophys. Res.*, *87*(A4), 2431–2443, doi:10.1029/JA087iA04p02431.
- Chang, S.-W., et al. (1998), A comparison of a model for the theta aurora with observations from Polar, Wind, and SuperDARN, *J. Geophys. Res.*, *103*(A8), 17,367–17,390, doi:10.1029/97JA02255.
- Chiu, Y. T., N. U. Crooker, and D. J. Gorney (1985), Model of oval and polar cap arc configurations, *J. Geophys. Res.*, *90*(A6), 5153–5157, doi:10.1029/JA090iA06p05153.
- Cowley, S. W. H. (1981), Magnetospheric asymmetries associated with the Y-component of the IMF, *Planet. Space Sci.*, *29*, 79–96, doi:10.1016/0032-0633(81)90141-0.
- Craven, J. D., and L. A. Frank (1991), Diagnosis of auroral dynamics using global auroral imaging with emphasis on large-scale evolution, in *Auroral Physics*, edited by C.-I. Meng, M. J. Rycroft, and L. A. Frank, pp. 273–288, Cambridge Univ. Press, Cambridge, U. K.
- Craven, J. D., L. A. Frank, C. T. Russell, E. J. Smith, and R. P. Lepping (1986), Global auroral responses to magnetospheric compressions by shocks in the solar wind: Two case studies, in *Solar Wind-Magnetosphere Coupling*, edited by Y. Kamide and J. A. Slavin, pp. 367–380, Terra Sci., Tokyo.
- Craven, J. D., J. S. Murphree, L. A. Frank, and L. L. Cogger (1991), Simultaneous optical observations of transpolar arcs in the two polar caps, *Geophys. Res. Lett.*, *18*(12), 2297–2300, doi:10.1029/91GL02308.
- Crooker, N. U., and F. J. Rich (1993), Lobe cell convection as a summer phenomenon, *J. Geophys. Res.*, *98*(A8), 13,403–13,407, doi:10.1029/93JA01037.
- Cumnock, J. A., and L. G. Blomberg (2004), Transpolar arc evolution and associated potential patterns, *Ann. Geophys.*, *22*, 1213–1231, doi:10.5194/angeo-22-1213-2004.
- Cumnock, J. A., J. R. Sharber, R. A. Heelis, M. R. Hairston, and J. D. Craven (1997), Evolution of the global aurora during positive IMF  $B_Z$  and varying IMF  $B_Y$  conditions, *J. Geophys. Res.*, *102*(A8), 17,489–17,497, doi:10.1029/97JA01182.
- Davis, T. N. (1963), Negative correlation between polar cap visual auroral and magnetic activity, *J. Geophys. Res.*, *68*(15), 4447–4453.
- Dungey, J. W. (1961), Interplanetary magnetic field and the auroral zones, *Phys. Rev. Lett.*, *6*(2), 47–48, doi:10.1103/PhysRevLett.6.47.
- Dungey, J. W. (1965), The length of the magnetospheric tail, *J. Geophys. Res.*, *70*(7), 1753–1753, doi:10.1029/JZ070i007p01753.
- Fairfield, D. H. (1979), On the average configuration of the geomagnetic tail, *J. Geophys. Res.*, *84*(A5), 1950–1958, doi:10.1029/JA084iA05p01950.
- Fairfield, D. H., R. P. Lepping, L. A. Frank, K. L. Ackerson, W. R. Paterson, S. Kokubun, T. Yamamoto, K. Tsuruda, and M. Nakamura (1996), Geotail observations of an unusual magnetotail under very northward IMF conditions, *J. Geomagn. Geoelectr.*, *48*, 473–487.
- Frank, L. A., J. D. Craven, J. L. Burch, and J. D. Winningham (1982), Polar views of the Earth’s aurora with Dynamics Explorer, *Geophys. Res. Lett.*, *9*(9), 1001–1004, doi:10.1029/GL009i009p1001.
- Frank, L. A., et al. (1986), The theta aurora, *J. Geophys. Res.*, *91*(A3), 3177–3224, doi:10.1029/JA091iA03p03177.
- Goudarzi, A., M. Lester, S. E. Milan, and H. U. Frey (2008), Multi-instrumentation observations of a transpolar arc in the northern hemisphere, *Ann. Geophys.*, *26*, 201–210, doi:10.5194/angeo-26-201-2008.
- Gusev, M. G., and O. A. Troshichev (1986), Hook-shaped arcs in day-side polar cap and their relation to the IMF, *Planet. Space Sci.*, *34*(6), 489–496, doi:10.1016/0032-0633(86)90087-5.

- Gussenhoven, M. S. (1982), Extremely high latitude auroras, *J. Geophys. Res.*, *87*(A4), 2401–2412, doi:10.1029/JA087iA04p02401.
- Hosokawa, K., J. I. Moen, K. Shiokawa, and Y. Otsuka (2011), Motion of polar cap arcs, *J. Geophys. Res.*, *116*, A01305, doi:10.1029/2010JA015906.
- Kan, J. R., and W. J. Burke (1985), A theoretical model of polar cap auroral arcs, *J. Geophys. Res.*, *90*(A5), 4171–4177, doi:10.1029/JA090iA05p04171.
- King, J. H., and N. E. Papitashvili (2005), Solar wind spatial scales in and comparisons of hourly Wind and ACE plasma and magnetic field data, *J. Geophys. Res.*, *110*, A02104, doi:10.1029/2004JA010649.
- Kullen, A. (2000), The connection between transpolar arcs and magnetotail rotation, *Geophys. Res. Lett.*, *27*(1), 73–76, doi:10.1029/1999GL010675.
- Kullen, A., M. Brittnacher, J. A. Cumnock, and L. G. Blomberg (2002), Solar wind dependence of the occurrence and motion of polar auroral arcs: A statistical study, *J. Geophys. Res.*, *107*(A11), 1362, doi:10.1029/2002JA009245.
- Lavraud, B., M. F. Thomsen, M. G. G. T. Taylor, Y. L. Wang, T. D. Phan, S. J. Schwartz, R. C. Elphic, A. Fazakerley, H. Rème, and A. Balogh (2005), Characteristics of the magnetosheath electron boundary layer under northward interplanetary magnetic field: Implications for high-latitude reconnection, *J. Geophys. Res.*, *110*, A06209, doi:10.1029/2004JA010808.
- Lyons, L. R. (1985), A simple model for polar cap convection patterns and generation of  $\theta$  auroras, *J. Geophys. Res.*, *90*(A2), 1561–1567, doi:10.1029/JA090iA02p01561.
- Makita, K., C.-I. Meng, and S.-I. Akasofu (1991), Transpolar auroras, their particle precipitation, and IMF  $B_Y$  component, *J. Geophys. Res.*, *96*(A8), 14,085–14,095, doi:10.1029/90JA02323.
- Mawson, D. (1925), *Scientific Reports (Australasian Antarctic Expedition (1911–1914)): Series B*, Gov. Printer, Sydney, Australia.
- Mende, S. B., et al. (2000a), Far ultraviolet imaging from the IMAGE spacecraft: 1. System design, *Space Sci. Rev.*, *91*, 243–270, doi:10.1023/A:1005271728567.
- Mende, S. B., et al. (2000b), Far ultraviolet imaging from the IMAGE spacecraft: 2. Wideband FUV imaging, *Space Sci. Rev.*, *91*, 271–285, doi:10.1023/A:1005227915363.
- Mende, S. B., et al. (2000c), Far ultraviolet imaging from the IMAGE spacecraft: 3. Spectral imaging of Lyman- $\alpha$  and OI 135.6 nm, *Space Sci. Rev.*, *91*, 287–318, doi:10.1023/A:1005292301251.
- Milan, S. E., S. W. H. Cowley, M. Lester, D. M. Wright, J. A. Slavin, M. Fillingim, C. W. Carlson, and H. J. Singer (2004), Response of the magnetotail to changes in the open flux content of the magnetosphere, *J. Geophys. Res.*, *109*, A04220, doi:10.1029/2003JA010350.
- Milan, S. E., B. Hubert, and A. Grocott (2005), Formation and motion of a transpolar arc in response to dayside and nightside reconnection, *J. Geophys. Res.*, *110*, A01212, doi:10.1029/2004JA010835.
- Milan, S. E., G. Provan, and B. Hubert (2007), Magnetic flux transport in the Dungey cycle: A survey of dayside and nightside reconnection rates, *J. Geophys. Res.*, *112*, A01209, doi:10.1029/2006JA011642.
- Milan, S. E., A. Grocott, and B. Hubert (2010), A superposed epoch analysis of auroral evolution during substorms: Local time of onset region, *J. Geophys. Res.*, *115*, A00104, doi:10.1029/2010JA015663.
- Newell, P. T., and C.-I. Meng (1995), Creation of theta-auroras: The isolation of plasma sheet fragments in the polar cap, *Science*, *270*(5240), 1338–1341, doi:10.1126/science.270.5240.1338.
- Newell, P. T., D. Xu, C.-I. Meng, and M. G. Kivelson (1997), Dynamical polar cap: A unifying approach, *J. Geophys. Res.*, *102*(A1), 127–139, doi:10.1029/96JA03045.
- Østgaard, N., S. B. Mende, H. U. Frey, L. A. Frank, and J. B. Sigwarth (2003), Observations of non-conjugate theta aurora, *Geophys. Res. Lett.*, *30*(21), 2125, doi:10.1029/2003GL017914.
- Peterson, W. K., and E. G. Shelley (1984), Origin of the plasma in a cross-polar cap auroral feature (theta aurora), *J. Geophys. Res.*, *89*(A8), 6729–6736, doi:10.1029/JA089iA08p06729.
- Reiff, P. H., and J. L. Burch (1985), IMF  $B_Y$ -dependent plasma flow and Birkeland currents in the dayside magnetosphere: 2. A global model for northward and southward IMF, *J. Geophys. Res.*, *90*(A2), 1595–1609, doi:10.1029/JA090iA02p01595.
- Rezhnev, B. V. (1995), A possible mechanism for  $\theta$  aurora formation, *Ann. Geophys.*, *13*(7), 698–703, doi:10.1007/s00585-995-0698-3.
- Sojka, J. J., L. Zhu, D. J. Crain, and R. W. Schunk (1994), Effect of high-latitude ionospheric convection on Sun-aligned polar caps, *J. Geophys. Res.*, *99*(A5), 8851–8863, doi:10.1029/93JA02667.
- Toffoletto, F. R., and T. W. Hill (1989), Mapping of the solar wind electric field to the Earth's polar caps, *J. Geophys. Res.*, *94*(A1), 329–347, doi:10.1029/JA094iA01p00329.
- Tsyganenko, N. A. (1989), A magnetospheric magnetic field model with a warped tail current sheet, *Planet. Space Sci.*, *37*(1), 5–20, doi:10.1016/0032-0633(89)90066-4.
- Valladares, C. E., H. C. Carlson, and K. Fukui (1994), Interplanetary magnetic field dependency of stable Sun-aligned polar cap arcs, *J. Geophys. Res.*, *99*(A4), 6247–6272, doi:10.1029/93JA03255.
- Walker, R. J., R. L. Richard, T. Ogino, and M. Ashour-Abdalla (1999), The response of the magnetotail to changes in the IMF orientation: The magnetotail's long memory, *Phys. Chem. Earth, Part C*, *24*(1–3), 221–227, doi:10.1016/S1464-1917(98)00032-4.
- Weill, G. (1958), Aspects de l'aurora observée à la base Dumont-d'Urville en Terre Adélie, *C. R. Hebd. Seances Acad. Sci.*, *246*, 2925–2927.
- Zhu, L., R. W. Schunk, and J. J. Sojka (1997), Polar cap arcs: A review, *J. Atmos. Terr. Phys.*, *59*(10), 1087–1126, doi:10.1016/S1364-6826(96)00113-7.

---

R. C. Fear and S. E. Milan, Department of Physics and Astronomy, University of Leicester, University Road, Leicester LE1 7RH, UK. (r.fear@ion.le.ac.uk)